

Cite this: *Green Chem.*, 2019, **21**, 6252

Received 18th September 2019,
Accepted 30th October 2019

DOI: 10.1039/c9gc03277k

rsc.li/greenchem

Biomass-derived N-doped porous carbon: an efficient metal-free catalyst for methylation of amines with CO₂†

Feiyang Tang,^a Liqiang Wang^{a,b} and You-Nian Liu^{a,b}

Developing green, efficient, and low-cost catalysts for methylation of N–H by using CO₂ as the C1 resource is highly desired yet remains a significant challenge. Herein, N-doped porous carbons (NPCs) were designed, synthesized, and proved to be an excellent metal-free catalyst for CO₂-participated methylation conversion. NPCs were prepared *via* the pyrolysis of a mixture of tannic acid and urea. Both theoretical calculation and experiment demonstrate that the N species especially pyridinic N and pyrrolic N within NPCs can work as Lewis basic sites for attacking CO₂ to weaken the C=O bonds and lower the molecule conversion barrier, facilitating the subsequent methylation of N–H to produce, for example, *N,N*-dimethylaniline. Besides, the unique porous structure can enrich CO₂ and accelerate mass transfer, synergistically promoting the conversion of CO₂. The optimized NPC_(1/5) catalyst, integrating the porous structure and strong Lewis basicity, exhibits excellent catalytic activity for CO₂-based methylation reaction under mild conditions (1 bar CO₂, 75 °C). Our work, for the first time, demonstrates the feasibility of using NPCs to catalyze the methylation of amino compounds to produce *N,N*-dimethylaniline by exploiting CO₂ as the C1 resource.

Carbon dioxide (CO₂) is the major greenhouse gas causing global warming, while it is also regarded as an inexpensive, non-toxic and sustainable C1 resource for the synthesis of high value-added fine chemicals and fuels.^{1–4} Compared with conventional capture and storage of CO₂, fixation and conversion of CO₂ is more attractive and economical considering that it can not only reduce the emission of CO₂ but also make full use of the C1 resource.^{5–8} Among various chemical approaches towards CO₂ utilization, methylation using CO₂ as the C1 resource for the construction of the C–N bond is proved to be

a promising and efficient route.^{9,10} In particular, methylation of N–H using CO₂ as the carbon resource can give rise to *N,N*-dimethylamine, which is broadly used in the synthesis of medicines, agrochemicals, perfumes, dyes and so on.^{11–15} To date, diverse catalysts have been developed to promote CO₂-participated methylation reaction (Fig. 1a), including organometallic catalysts,^{16–18} organic catalysts,^{19–22} inorganic bases^{23,24} and heterogeneous metallic catalysts.^{25–27} However, the problems of metal residues and separation limit the wide applications of these catalysts. In particular, metals are non-renewable and even toxic.^{28,29} Therefore, metal-free heterogeneous catalysts are much more attractive for CO₂-participated methylation reaction.

The big challenge facing CO₂ conversion is to activate the highly stable C=O bond of CO₂.³⁰ According to previous reports, a Lewis base bearing the ability to donate electrons can activate CO₂, as a Lewis acid, *via* a nucleophilic reaction-like pathway. For example, CO₂ can interact with DBU (1,8-diazabicyclo[5.4.0]undec-7-ene, a typical Lewis base) to form a carbonate-like species, which can significantly weaken the C=O

^aCollege of Chemistry and Chemical Engineering, Central South University, Changsha, Hunan 410083, P.R. China

^bState Key Laboratory of Powder Metallurgy, Central South University, Changsha, Hunan 410083, P.R. China. E-mail: liqiangwang@csu.edu.cn, liuyounian@csu.edu.cn

† Electronic supplementary information (ESI) available. See DOI: 10.1039/c9gc03277k

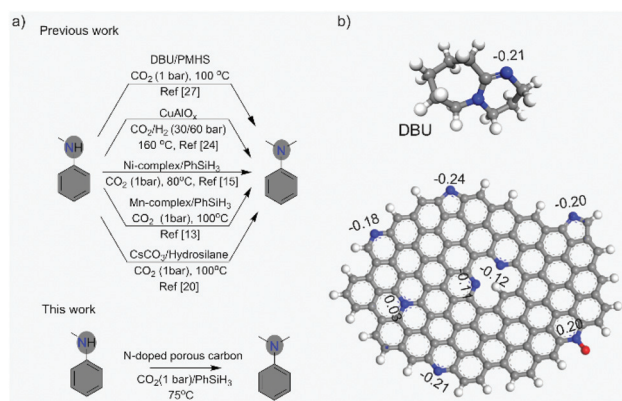


Fig. 1 (a) Previously and newly proposed routes for methylation of N–H using CO₂ as a C1 source. (b) Hirshfeld charge population analysis of DBU and a simulated NPC model.

bond and lower the CO₂ conversion energy barrier.^{31,32} Due to their tunable structure and composition, high stability, and excellent conductivity, N-doped porous carbon materials have attracted wide attention in catalysis.^{33–35} Notably, N-species within carbon matrices, especially pyridinic N and pyrrolic N, can act as a Lewis basic site to activate the contacted molecules and hence to promote their catalytic conversion.^{36,37} Besides, the porous structure favors mass transfer, allowing the reactants and products to transfer smoothly within the catalysts.³⁸ In addition, for the gas-involved reaction, the porous structure can enrich the gas molecules, which is kinetically beneficial for the catalytic reaction.^{39,40} Hence, we envisioned that N-doped, porous carbon materials could act as metal-free heterogeneous catalysts to activate CO₂ for the subsequent methylation reaction to produce *N,N*-dimethylamine. To the best of our knowledge, there have been no reports on using NPC catalysts for methylation of amines with CO₂.

Herein, through theoretical computation with DBU as a reference Lewis base, we verified that pyridinic N and pyrrolic N within the N-doped carbon matrices exhibit considerable Lewis basicity. They could interact with CO₂ to weaken the C=O bond, facilitating the following methylation reaction. Then, a series of N-doped, porous carbon materials (NPCs) were prepared *via* carbonizing the mixture of urea and tannic acid with different mass ratios. NPCs possess a hierarchically porous structure and N-dopant induced Lewis basic sites. The unique structure and composition could significantly lower the conversion barrier of CO₂ and further promote methylation. NPCs can efficiently catalyze the methylation of *N*-methylaniline with CO₂ for the synthesis of *N,N*-substituted amine derivatives within a range of CO₂ concentrations from 100% to 20% (CO₂:N₂) under mild conditions (1 bar, 75 °C). The excellent performance of NPCs is due to the strong CO₂ affinity and their porous structure.

Firstly, the theoretical calculation was performed to demonstrate that NPCs are a qualified candidate for heterogeneous Lewis basic catalysts, using DBU as a reference (a widely exploited homogeneous Lewis basic catalyst). The Lewis basicity can be determined from the electron-donating capability, which can be evaluated through charge analysis.^{41,42} The N species of N-doped porous carbon mainly include graphitic N, pyridinic N, pyrrolic N and oxidized N (Fig. 1b). Graphitic N bonds with three carbon atoms, while pyridinic N (six-ring) and pyrrolic N (five-ring) bond with two carbon atoms. For oxidized N, the N atom bonds with an O atom. As shown in Fig. 1b, pyridinic N and pyrrolic N prefer to exist in the defect site and zigzag edge of carbon materials. The Hirshfeld charge population analysis of DBU and a NPC model is shown in Fig. 1b. It can be seen that the pyridinic N (−0.11 to −0.20) and pyrrolic N (−0.20 to −0.24) of NPCs possess excess negative charge which is similar to the active N site (−0.21) of DBU and this demonstrates that pyridinic N and pyrrolic N exhibit considerable Lewis basicity, while graphitic N and oxidized N possess positive charge (0.03 and 0.20), suggesting that they have negligible Lewis basicity. The Lewis basic sites can provide nucleophilic sites to interact with the C atom of CO₂

and hence to activate the CO₂ molecule, which often leads to the twist of molecule structure and the increase of bond length. Therefore, the molecular structure of CO₂ before and after interacting with the pyridinic N and pyrrolic N of NPCs was investigated. As shown in Fig. S1,† the initial bond length of C=O is 1.168 Å, and the angle of CO₂ is 180.0°. After interacting with the pyridinic N or pyrrolic N, the bond length of C=O changes to 1.175 Å and 1.178 Å, and the angle of the CO₂ molecule changes to 165.8° and 162.5°, respectively. The results demonstrate that the pyridinic N or pyrrolic N could interact with the CO₂ molecule to affect its molecular structure. Meanwhile, the longer bond length and smaller angle indicate lower bond energy, in favor of CO₂ activation and catalytic conversion. In addition, the pyrrolic N exhibits stronger interaction with the CO₂ molecule than the pyridinic N, arising from its higher negative charge. Interestingly, it was found that graphitic N could enhance the negative charge on pyridinic N or pyrrolic N (Fig. S2†). To sum up, it is theoretically possible for NPCs to work as metal-free heterogeneous catalysts for the activation of CO₂ to benefit the subsequent conversion.

Secondly, NPCs were prepared by carbonizing the dried mixing solution of urea and tannic acid (TA) with different mass ratios (Fig. 2a). The as-obtained NPCs exhibit typical (002) and (100) graphitic peaks at 25.2 and 43.4°, respectively (Fig. S3†). TEM and the corresponding HR-TEM images of different NPC samples are shown in Fig. 2b–i. All samples exhibit a similar sheet-like morphology. The porous structure can be deduced from the HR-TEM images, where there exist an interrupted crystal lattice and a defective structure (Fig. 2b–i). A closer observation shows that they are composed of ultra-thin nanosheets. The porous structure could indicate that NPCs are composed of stacked small pieces of carbon sheets,

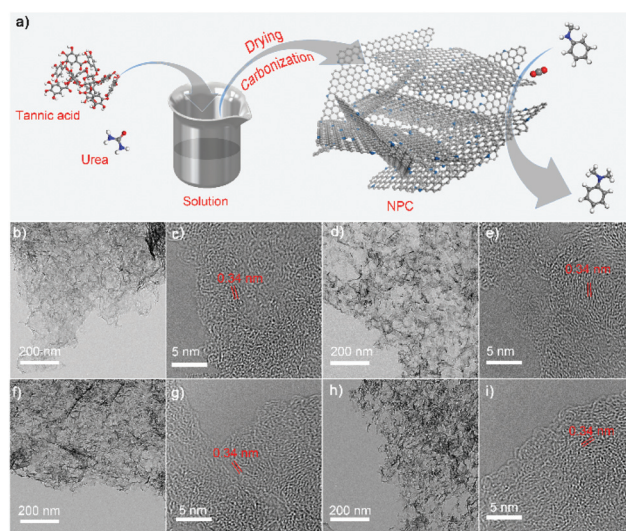


Fig. 2 (a) Synthesis of NPC. (b) XRD patterns of NPC samples. TEM and HRTEM images of (c and d) NPC_(1/2); (e and f) NPC_(1/3); (g and h) NPC_(1/5); and (i and k) NPC_(1/7).

which leads to plenty of large pores within the carbon matrices (Fig. S4†, highlighted in red lines). The unique 2D porous structure is highly desired in heterogeneous catalysis in view of exposing the active sites and promoting the mass transfer.

The chemical composition of the carbon surface was detected by XPS. The peaks of C, N and O can be found on the XPS spectrum (Fig. S6†), which agrees well with the energy-dispersive X-ray (EDX) mapping results, where a uniform N distribution is observed (Fig. S5†). The C 1s spectra can be divided into three different peaks, which are ascribed to the bond of C–C, C–N/C–O and C=O (Fig. S7†). The N 1s spectra of all samples are shown in Fig. 3a. The N 1s spectra can be divided into four different peaks that are graphitic N, pyridinic N, pyrrolic N and oxidized N.⁴³ The contents of different N species are listed in Table S1.† It can be found that the content of N increases from 7.6 at% to 8.3 at% with the increment of urea proportion. Specifically, NPC_(1/5) possesses a lower graphitic N content (2.7 at%) but higher pyrrolic N (0.7 at%) and pyridinic N (4.0 at%) contents than its companions (NPC_(1/2): 3.1 at%, 0.5 at% and 3.6 at%; NPC_(1/3): 3.4 at%, 0.5 at% and 3.1 at%; and NPC_(1/7): 3.5 at%, 0.5 at% and 3.8 at%). Of note, pyridinic N and pyrrolic N only exist in the zigzag edge or the defect site of N-doped carbon materials. This situation means that there exist defective structures within NPCs. Thus, Raman measurement was performed to obtain more information on the defective structure. As shown in Fig. 3b, the spectra exhibit two different peaks, the D band (at around 1340 cm⁻¹) and the G band (at around 1587 cm⁻¹), which are assigned to the disordered and graphitic nature of the carbon structure, respectively.²⁹ All samples possess a highly defective structure, and have a similar value of I_D/I_G: 1.01 (NPC_(1/2)), 1.05 (NPC_(1/3)), 1.02 (NPC_(1/5)) and 1.10 (NPC_(1/7)). The structural defect is often present along with the

porous structure. Thus, the porous property of the NPCs was investigated *via* the nitrogen adsorption/desorption isotherm and the pore size distribution (Fig. S8 and Table S2†). Interestingly, the N₂ adsorption and desorption isotherms display a remarkable increase at low pressure for all NPC samples, indicating the existence of micropores within them. Besides, the occurrence of hysteresis loops at P/P_0 of 0.5 to 0.9 suggests the presence of mesopores. The pore structure was further confirmed by the pore size distribution, where micropores with a size from 1 to 1.5 nm, mesopores with a size from 8 to 50 nm and even macropores (with a size >50 nm) were observed. The specific surface area (S_{BET}) follows the order of NPC_(1/2) (107.6 m² g⁻¹) < NPC_(1/3) (146.5 m² g⁻¹) < NPC_(1/5) (216.8 m² g⁻¹) < NPC_(1/7) (242.8 m² g⁻¹). The unique hierarchically porous structure can not only enrich CO₂, but also allow the CO₂ molecule to fully access the Lewis basic N sites, synergistically promoting the catalytic conversion of CO₂. Then, the CO₂ uptake ability of all NPC samples was investigated to determine their capacity for CO₂ enrichment. The CO₂ uptake amounts reach 44.5, 52.2, 62.8 and 54.4 mg g⁻¹ for NPC_(1/2), NPC_(1/3), NPC_(1/5) and NPC_(1/7), respectively, at 273 K and 1 bar, while, at 298 K and 1 bar, they are 31.6, 34.1, 39.2 and 40.9 mg g⁻¹, respectively (Fig. S9a†). The CO₂ uptake capacity of NPCs confirms the affinity of NPCs for CO₂, which is relevant to the basic N-sites. The adsorption heat for different NPCs is shown in Fig. S9b.† NPC_(1/5) exhibits the highest value, indicating its strongest CO₂ affinity. The affinity of NPCs to CO₂ can enhance the concentration of CO₂ in the pore channel of NPCs, kinetically favouring the conversion of CO₂. CO₂ TPD tests were further performed to prove that the introduced N can work as Lewis basic sites. There exists an obvious CO₂ signal for all NPCs within the temperature range from 375 to 500 K, which arises from the Lewis acid–base interaction.⁴⁴ As the types of N species and their contents vary with different samples, the interactions between them and CO₂ vary too, leading to the slight difference in desorption temperature. The total CO₂ signal strength for each sample was calculated *via* integrating the desorption curves from 375 to 500 K, and it follows the order of NPC_(1/5) (17) > NPC_(1/7) (14) > NPC_(1/3) (8) > NPC_(1/2) (3) (Fig. 3c). These suggest that NPC_(1/5) exhibits higher basicity and is possibly more active in the catalytic CO₂ conversion.

Thirdly, catalytic methylation of *N*-methylamine into *N,N*-dimethylamine using CO₂ as the C1 resource was taken as a model to evaluate the catalytic performance of the obtained NPCs. The detailed determination conditions of HPLC are shown in Fig. S10.† As shown in Table 1, hardly any *N*-methylamine (2.1%) was converted into *N,N*-dimethylamine in the absence of the catalyst in CH₃CN solution (entry 1). The conversion (*C*) of *N*-methylamine increases significantly in the presence of NPC catalysts and follows the order of NPC_(1/5) > NPC_(1/7) > NPC_(1/3) > NPC_(1/2). In particular, NPC_(1/5) performs the best with the highest conversion (80.1%), and the selectivity (*S*) goes up to 83.9%. The excellent catalytic performance could be ascribed to its high capacity for CO₂ uptake and strong Lewis basicity. Then, we investigated the impact of solvents (including CH₃OH, 1,4-dioxane, CH₃CN, THF, DMSO

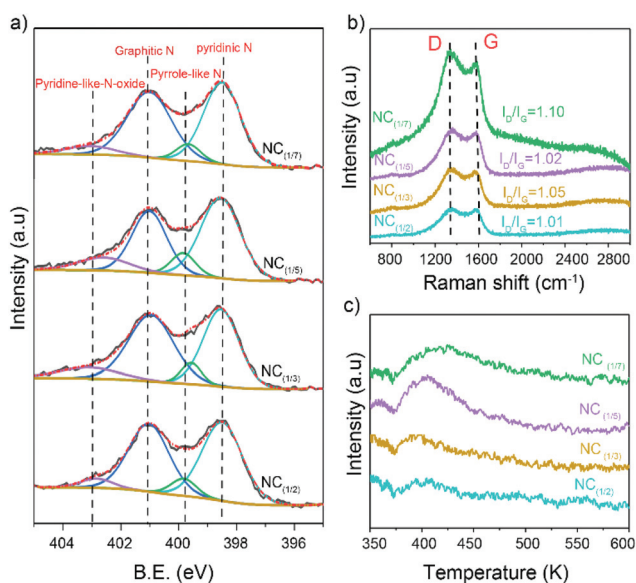


Fig. 3 (a) N 1s XPS spectra, (b) Raman spectra and (c) CO₂ TPD results of NPC_(1/2), NPC_(1/3), NPC_(1/5) and NPC_(1/7).

Table 1 Methylation reaction of *N*-methylaniline with CO₂ under various conditions

| Entry | Catalyst | <i>C</i> (%) | <i>S</i> (%) | |
|----------------|----------------------|--------------|--------------|-----------|
| | | | 1b | 1c |
| 1 | No catalyst | 2.1 | 83.0 | 17.0 |
| 2 | NPC _(1/2) | 25.7 | 81.2 | 18.8 |
| 3 | NPC _(1/3) | 39.6 | 80.0 | 20.0 |
| 4 | NPC _(1/5) | 80.1 | 83.9 | 16.1 |
| 5 | NPC _(1/7) | 65.8 | 87.0 | 13.0 |
| 6 ^a | NPC _(1/5) | 97.1 | 90.2 | 9.8 |
| 7 ^a | No catalyst | 64.1 | 78.9 | 21.1 |
| 8 ^b | No catalyst | 13.7 | 82.2 | 17.8 |
| 9 ^b | NPC _(1/5) | 71.3 | 86.6 | 13.4 |

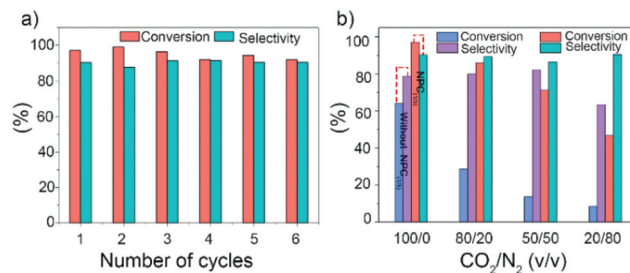
Reaction conditions: **1a** (0.25 mmol), PhSiH₃ (0.5 mmol), catalyst (15 mg), solvent (CH₃CN, 3 mL), 1 atm CO₂, 75 °C and 20 h. ^a Solvent was replaced by DMF, reaction time, 18 h. ^b Solvent was replaced by DMF, reaction time, 18 h, CO₂/N₂ (v/v, 1/1, 1 bar). Conversion (*C*) and selectivity (*S*) were determined by HPLC.

and DMF) on the catalytic performance (Table S3†). As expected, DMF of weak basicity performs the best of all (*C*: 97.1%, *S*: 90.2%). Of note, NPC_(1/5) even exhibits comparable catalytic activity to some of the recently reported homogeneous catalysts (listed in Table S4†). The kinetic data on the methylation reaction over NPC_(1/5) are shown in Fig. S11.† Under the optimized conditions, the methylation reaction was extended to other *N*-substituted amine derivatives. The corresponding products were obtained with high conversion and selectivity in both DMF and CH₃CN (Table 2). These methylation reactions were also carried out in the CH₃CN solvent (Table 2). The results further verify the high catalytic activity of NPC_(1/5), which arises from its intrinsic Lewis basicity and unique pore structure. Interestingly, when primary amine was utilized as a substrate for methylation reaction, the main product obtained was *N*-methylformanilide and its derivative (Scheme S1†). The recyclability and stability of NPC_(1/5) were also investigated *via* catalytic recycling measurements (Fig. 4a). After six catalytic runs, the catalyst shows a non-significant loss in catalytic activity (*C*: 92.1%, *S*: 90.5%), indicating its high recyclability under liquid phase reaction conditions. XPS tests were performed to determine the situation of the N active sites before and after the catalytic reaction. Neither the N types nor their content revealed obvious changes, which further confirms the catalytic stability of NPCs (Fig. S12 and Table S5†). As mentioned above, the NPCs show good CO₂ uptake capacity and abundant porosity, which allows CO₂ to be concentrated in pores even under low concentrations and favours its further conversion. The catalytic behaviour of NPC_(1/5) under different concentrations of CO₂ was further tested (Fig. 4b). Under 80% CO₂ concentration, the conversion of *N*-methylaniline was 86.2%, and the selectivity of *N,N*-dimethylaniline was 89.5%. When the CO₂ concentration dropped to 50%, the conversion

Table 2 Catalytic methylation of various *N*-substituted amines by NPC_(1/5)

| | | | |
|---|---|---|--|
|  |  |  |  |
| 1b: <i>C</i> : 97% <i>S</i> : 90% (<i>C</i> : 80.1% <i>S</i> : 83.9%) ^a | 2b: <i>C</i> : 83% <i>S</i> : 99% (<i>C</i> : 88.1% <i>S</i> : 92.0%) ^a | 3b: <i>C</i> : 96% <i>S</i> : 97% (<i>C</i> : 81.5% <i>S</i> : 87.2%) ^a | 4b: <i>C</i> : 90% <i>S</i> : 98% (<i>C</i> : 86.3% <i>S</i> : 88.2%) ^a |
|  |  |  |  |
| 5b: <i>C</i> : 98% <i>S</i> : 99% (<i>C</i> : 91.7% <i>S</i> : 97.5%) ^a | 6b: <i>C</i> : 94% <i>S</i> : 99% (<i>C</i> : 87.1% <i>S</i> : 94.8%) ^a | 7b: <i>C</i> : 93% <i>S</i> : 94% (<i>C</i> : 81.6% <i>S</i> : 92.5%) ^a | 8b: <i>C</i> : 92% <i>S</i> : 99% (<i>C</i> : 95.0% <i>S</i> : 86.2%) ^a |
|  |  |  | |
| 9b: <i>C</i> : 91% <i>S</i> : 99% (<i>C</i> : 97.7% <i>S</i> : 88.3%) ^a | 10b: <i>C</i> : 88% <i>S</i> : 94% (<i>C</i> : 87.2% <i>S</i> : 92.2%) ^a | 11b: <i>C</i> : 89% <i>S</i> : 93% (<i>C</i> : 74.5% <i>S</i> : 89.1%) ^a | |
|  |  | | |
| 12b: <i>C</i> : 84% <i>S</i> : 88% (<i>C</i> : 82.6% <i>S</i> : 92.8%) ^a | 13b: <i>C</i> : 78% <i>S</i> : 94% (<i>C</i> : 75.1% <i>S</i> : 91.4%) ^a | | |

Reaction conditions: Reactant (0.25 mmol), PhSiH₃ (0.5 mmol), catalyst (15 mg), solvent (DMF, 3 mL). ^a Solvent was replaced by CH₃CN. Conversion (*C*) and selectivity (*S*) were determined by HPLC.

**Fig. 4** (a) The recycling experiments for NPC_(1/5). (b) The catalytic performance in the absence and presence of NPC_(1/5) under various CO₂ concentrations.

and selectivity were 71.3% and 86.6%, respectively. Even when the CO₂ concentration was decreased to 20%, they remained at 46.8% (*C*) and 90.6% (*S*), respectively. In the absence of NPC_(1/5), the DMF solvent showed much more inferior performance, especially under relatively lower concentrations of CO₂. This finding further confirms the high activity of NPCs, which can be strengthened by the DMF solvent due to its Lewis basicity. The superior catalytic performance in the presence of NPC_(1/5) possibly comes from the high porosity and CO₂ affinity of NPC_(1/5), which ensures relatively high CO₂ concentration in the porous channel even under relatively low CO₂ concentrations.

Lastly, the theoretical calculation was presented to understand the mechanism of Lewis basic N species catalysed CO₂-participated methylation reaction. As mentioned above, NPCs exhibit strong Lewis basicity, and the Lewis basic sites can

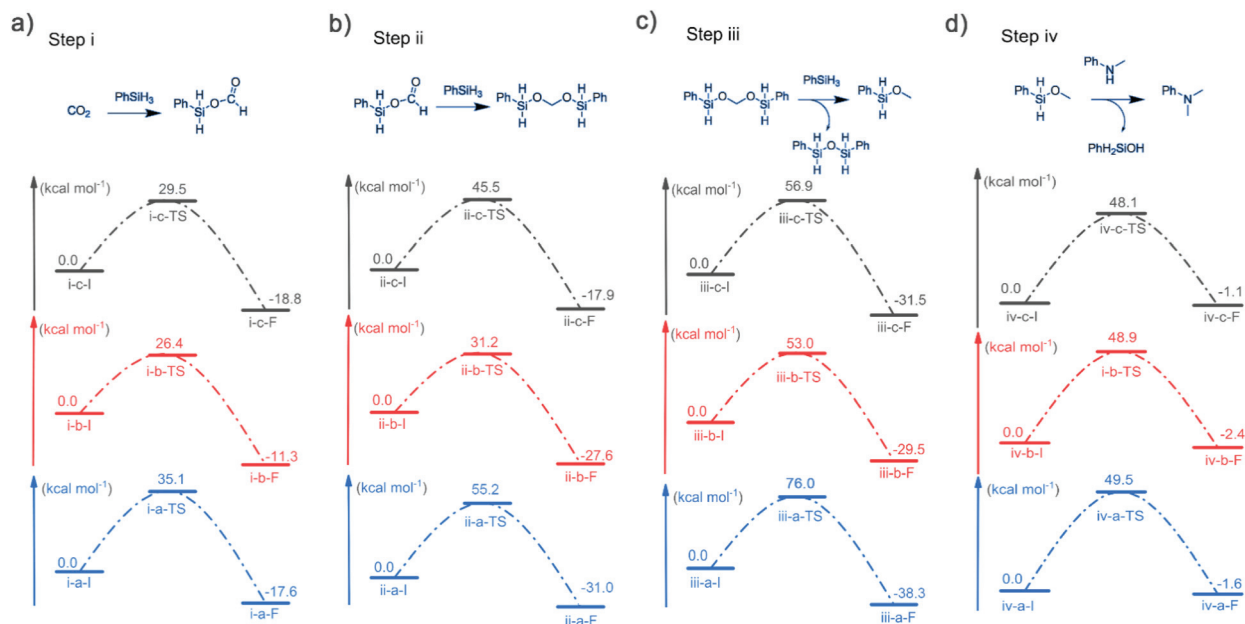


Fig. 5 Energy profile for CO_2 -participated methylation reaction. (a) Step i, (b) step ii, (c) step iii, and (d) step iv. In the absence of the catalyst (blue), in the presence of the pyridinic N site (red), and in the presence of the pyrrolic N site (grey). I, TS and F represent the initial state, the transition state and the final state, respectively.

interact with CO_2 to polarize the CO_2 molecules, which is supposed to loosen the $\text{C}=\text{O}$ bond, lower the energy barrier for breaking the $\text{C}=\text{O}$ bond, and hence benefit the catalytic conversion of CO_2 . Based on previous reports,^{14,23,45,46} the process of CO_2 -participated methylation reaction mainly involves four steps (Scheme S2[†]): (i) hydrosilylation of CO_2 to form silyl formates; (ii) hydrosilylation of silyl formates to form silyl acetals; (iii) intermolecular hydrosilylation to form silylmethoxide species; and (iv) methylation of amines with silylmethoxide to yield the methylated products. Herein, by means of theoretical calculation, we analysed the reaction process of CO_2 -participated methylation in the absence or presence of different Lewis basic N species (pyridinic N and pyrrolic N). In step (i), in the absence of N species, the energy barrier of the reaction between PhSiH_3 and CO_2 is $35.1 \text{ kcal mol}^{-1}$, while in the presence of pyridinic N and pyrrolic N, the energy barrier drops to 26.4 and $29.5 \text{ kcal mol}^{-1}$, respectively (Fig. 5a and Fig. S13[†]). These results indicate that Lewis basic N sites could significantly activate CO_2 and lower its conversion barrier, promoting the reaction of CO_2 with PhSiH_3 . In step (ii), in the presence of pyridinic N and pyrrolic N, the energy barrier drops from 55.2 to 31.2 and $45.5 \text{ kcal mol}^{-1}$, respectively (Fig. 5b and Fig. S14[†]). In step (iii), the energy barrier declines from 76.0 to 53.0 and $56.9 \text{ kcal mol}^{-1}$ in the presence of pyridinic N and pyrrolic N, respectively (Fig. 5c and Fig. S15[†]). In contrast, in step (iv), non-obvious changes in the energy barrier were observed (Fig. 5d and Fig. S16[†]). The Lewis basic N species play an important role in steps (i) to (iii) to lower the reaction barriers. Consequently, the presence of Lewis basic N species could significantly promote the methylation with CO_2 .

Conclusions

In summary, N-doped porous carbons (NPCs), which were prepared by direct pyrolysis of the mixture of tannic acid and urea, were developed as a metal-free catalyst for CO_2 -participated catalytic methylation reaction. The N species especially pyrrolic N and pyridinic N within the carbon matrices afford NPCs strong Lewis basicity. The N species can work as nucleophilic sites to attack the C atom of CO_2 , weakening the $\text{C}=\text{O}$ bond and hence lowering the energy barrier for CO_2 conversion. Besides, the hierarchical porous structure of NPCs can help to enrich CO_2 and accelerate mass transfer, which kinetically favors the CO_2 -participated methylation conversion. As a result, $\text{NPC}_{(1/5)}$ shows high catalytic activity, selectivity and stability, and can efficiently catalyze the methylation of N–H into *N,N*-dimethylamine using CO_2 as the C1 resource under mild conditions. Our work, for the first time, proved the feasibility of using N-doped, porous carbon as an efficient metal-free catalyst for methylation reaction using CO_2 as the C1 resource.

Conflicts of interest

There are no conflicts to declare.

Acknowledgements

This work was supported by the National Natural Science Foundation of China (No. 21636010 and 21878342), the China

Postdoctoral Science Foundation (2018M643001), Hunan Provincial Natural Science Foundation of China (No. 2019JJ50758), the Postdoctoral Science Foundation of Central South University (No. 205440), and the State Key Laboratory of Powder Metallurgy, Central South University, Changsha, China and the Fundamental Research Funds for Central Universities of Central South University (No. 2018zzts114).

Notes and references

- Q.-W. Song, Z.-H. Zhou and L.-N. He, *Green Chem.*, 2017, **19**, 3707–3728.
- F. Tang, J. Hou, K. Liang, J. Huang and Y.-N. Liu, *Eur. J. Inorg. Chem.*, 2018, **2018**, 4175–4180.
- X. Yu, Z. Yang, B. Qiu, S. Guo, P. Yang, B. Yu, H. Zhang, Y. Zhao, X. Yang, B. Han and Z. Liu, *Angew. Chem., Int. Ed.*, 2019, **58**, 632–636.
- B. B. A. Bediako, Q. Qian, J. Zhang, Y. Wang, X. Shen, J. Shi, M. Cui, G. Yang, Z. Wang, S. Tong and B. Han, *Green Chem.*, 2019, **21**, 4152–4158.
- M. A. A. Aziz, A. A. Jalil, S. Triwahyono and A. Ahmad, *Green Chem.*, 2015, **17**, 2647–2663.
- A. J. Kamphuis, F. Picchioni and P. P. Pescarmona, *Green Chem.*, 2019, **21**, 406–448.
- M. North, *ChemSusChem*, 2019, **12**, 1763–1765.
- Y. Wang, S. Li, Y. Yang, X. Shen, H. Liu and B. Han, *Chem. Commun.*, 2019, **55**, 6942–6945.
- G. Yan, A. J. Borah, L. Wang and M. Yang, *Adv. Synth. Catal.*, 2015, **357**, 1333–1350.
- R. A. Pramudita and K. Motokura, *Green Chem.*, 2018, **20**, 4834–4843.
- W. Zhao, X. Chi, H. Li, J. He, J. Long, Y. Xu and S. Yang, *Green Chem.*, 2019, **21**, 567–577.
- Z. Guo, B. Zhang, X. Wei and C. Xi, *ChemSusChem*, 2018, **11**, 2296–2299.
- A. Gopakumar, I. Akçok, L. Lombardo, F. Le Formal, A. Magrez, K. Sivula and P. J. Dyson, *ChemistrySelect*, 2018, **3**, 10271–10276.
- H. Niu, L. Lu, R. Shi, C. W. Chiang and A. Lei, *Chem. Commun.*, 2017, **53**, 1148–1151.
- H. Lv, Q. Xing, C. Yue, Z. Lei and F. Li, *Chem. Commun.*, 2016, **52**, 6545–6548.
- Z. Huang, X. Jiang, S. Zhou, P. Yang, C. X. Du and Y. Li, *ChemSusChem*, 2019, **12**, 3054–3059.
- R. H. Lam, C. M. A. McQueen, I. Pernik, R. T. McBurney, A. F. Hill and B. A. Messerle, *Green Chem.*, 2019, **21**, 538–549.
- L. González-Sebastián, M. Flores-Alamo and J. J. García, *Organometallics*, 2015, **34**, 763–769.
- W. C. Chen, J. S. Shen, T. Jurca, C. J. Peng, Y. H. Lin, Y. P. Wang, W. C. Shih, G. P. Yap and T. G. Ong, *Angew. Chem., Int. Ed.*, 2015, **54**, 15207–15212.
- S. Das, F. D. Bobbink, G. Laurenczy and P. J. Dyson, *Angew. Chem., Int. Ed.*, 2014, **53**, 12876–12879.
- X. F. Liu, X. Y. Li, C. Qiao, H. C. Fu and L. N. He, *Angew. Chem., Int. Ed.*, 2017, **56**, 7425–7429.
- Y. Lu, Z. H. Gao, X. Y. Chen, J. Guo, Z. Liu, Y. Dang, S. Ye and Z. X. Wang, *Chem. Sci.*, 2017, **8**, 7637–7650.
- C. Fang, C. Lu, M. Liu, Y. Zhu, Y. Fu and B.-L. Lin, *ACS Catal.*, 2016, **6**, 7876–7881.
- X.-D. Li, S.-M. Xia, K.-H. Chen, X.-F. Liu, H.-R. Li and L.-N. He, *Green Chem.*, 2018, **20**, 4853–4858.
- X. Cui, Y. Zhang, Y. Deng and F. Shi, *Chem. Commun.*, 2014, **50**, 13521–13524.
- T. Toyao, S. M. A. H. Siddiki, K. Ishihara, K. Kon, W. Onodera and K. Shimizu, *Chem. Lett.*, 2017, **46**, 68–70.
- X. Cui, X. Dai, Y. Zhang, Y. Deng and F. Shi, *Chem. Sci.*, 2014, **5**, 649–655.
- D. Su, G. Wen, Q. Gu, Y. Liu, R. Schlogl, C. Wang and Z. Tian, *Angew. Chem., Int. Ed.*, 2018, **57**, 16898–16902.
- F. Y. Tang, L. Q. Wang, G. J. Zhang, M. Zhang and Y.-N. Liu, *Ind. Eng. Chem. Res.*, 2019, **58**, 5543–5551.
- Z. Ke, L. Hao, X. Gao, H. Zhang, Y. Zhao, B. Yu, Z. Yang, Y. Chen and Z. Liu, *Chem. – Eur. J.*, 2017, **23**, 9721–9725.
- G. Li, J. Chen, D.-Y. Zhu, Y. Chen and J.-B. Xia, *Adv. Synth. Catal.*, 2018, **360**, 2364–2369.
- Y. Jiang, O. Blacque, T. Fox and H. Berke, *J. Am. Chem. Soc.*, 2013, **135**, 7751–7760.
- L. Wang, K. Liang, L. Deng and Y.-N. Liu, *Appl. Catal., B*, 2019, **246**, 89–99.
- L. Wang, X. Jiang, M. Zhang, M. Yang and Y.-N. Liu, *Chem. – Asian J.*, 2017, **12**, 2374–2378.
- K. Liang, Y. Xu, L. Wang, Y. Liu and Y.-N. Liu, *ChemCatChem*, 2019, **11**, 4822–4829.
- D. Guo, R. Shibuya, C. Akiba, S. Saji, T. Kondo and J. Nakamura, *Science*, 2016, **351**, 361–365.
- J. Wu, C. Wen, X. Zou, J. Jimenez, J. Sun, Y. Xia, M.-T. F. Rodrigues, S. Vinod, J. Zhong, N. Chopra, I. N. Odeh, G. Ding, J. Lauterbach and P. M. Ajayan, *ACS Catal.*, 2017, **7**, 4497–4503.
- W. Xing, C. Liu, Z. Zhou, L. Zhang, J. Zhou, S. Zhuo, Z. Yan, H. Gao, G. Wang and S. Z. Qiao, *Energy Environ. Sci.*, 2012, **5**, 7323–7327.
- Z. J. Mu, X. Ding, Z. Y. Chen and B. H. Han, *ACS Appl. Mater. Interfaces*, 2018, **10**, 41350–41358.
- B. Dong, L. Wang, S. Zhao, R. Ge, X. Song, Y. Wang and Y. Gao, *Chem. Commun.*, 2016, **52**, 7082–7085.
- Y. Liu, J. Zhao and Q. Cai, *Phys. Chem. Chem. Phys.*, 2016, **18**, 5491–5498.
- T.-Z. Hou, H.-J. Peng, J.-Q. Huang, Q. Zhang and B. Li, *2D Mater.*, 2015, **2**, 014011–014017.
- J. Sheng, L. Wang, L. Deng, M. Zhang, H. He, K. Zeng, F. Tang and Y. N. Liu, *ACS Appl. Mater. Interfaces*, 2018, **10**, 7191–7200.
- J. Kim, S.-N. Kim, H.-G. Jang, G. Seo and W.-S. Ahn, *Appl. Catal., A*, 2013, **453**, 175–180.
- W. Li and C. K. Kim, *Bull. Korean Chem. Soc.*, 2017, **38**, 12–18.
- Y. Li, X. Cui, K. Dong, K. Junge and M. Beller, *ACS Catal.*, 2017, **7**, 1077–1086.